ESC European Society of Cardiology

Cardiovascular Research (2021) **117**, 1325–1338
doi:10.1093/cvr/cvaa221

Low-intensity pulsed ultrasound ameliorates cardiac diastolic dysfunction in mice: a possible novel therapy for heart failure with preserved left ventricular ejection fraction

Yuto Monma[1], Tomohiko Shindo[1], Kumiko Eguchi[1], Ryo Kurosawa [1], Yuta Kagaya[1], Yosuke Ikumi[1], Sadamitsu Ichijo [1], Takashi Nakata[1], Satoshi Miyata [2], Ayana Matsumoto[3], Haruka Sato[3], Masahito Miura[3], Hiroshi Kanai [4,5], and Hiroaki Shimokawa [1]*

[1]Department of Cardiovascular Medicine, Tohoku University Graduate School of Medicine, 1-1 Seiryo-machi, Aoba-ku, Sendai 980-8574, Japan; [2]Department of Evidence-Based Cardiovascular Medicine, Tohoku University Graduate School of Medicine, Sendai, Japan; [3]Department of Clinical Physiology, Tohoku University Graduate School of Medicine, Sendai, Japan; [4]Department of Electronic Engineering, Tohoku University Graduate School of Engineering, Sendai, Japan; and [5]Division of Biomedical Measurements and Diagnostics, Tohoku University Graduate School of Biomedical Engineering, Sendai, Japan

Received 9 April 2020; revised 30 May 2020; editorial decision 26 June 2020; accepted 14 July 2020; online publish-ahead-of-print 19 July 2020

Aims Heart failure with preserved left ventricular ejection fraction (HFpEF) is a serious health problem worldwide, as no effective therapy is yet available. We have previously demonstrated that our low-intensity pulsed ultrasound (LIPUS) therapy is effective and safe for angina and dementia. In this study, we aimed to examine whether the LIPUS therapy also ameliorates cardiac diastolic dysfunction in mice.

Methods and results Twelve-week-old obese diabetic mice (db/db) and their control littermates (db/+) were treated with either the LIPUS therapy [1.875 MHz, 32 cycles, Ispta (spatial peak temporal average intensity) 117–162 mW/cm^2, 0.25 W/cm^2] or placebo procedure two times a week for 4 weeks. At 20-week-old, transthoracic echocardiography and invasive haemodynamic analysis showed that cardiac diastolic function parameters, such as e′, *E*/e′, end-diastolic pressure–volume relationship, Tau, and d*P*/d*t* min, were all deteriorated in placebo-treated db/db mice compared with db/+ mice, while systolic function was preserved. Importantly, these cardiac diastolic function parameters were significantly ameliorated in the LIPUS-treated db/db mice. We also measured the force (F) and intracellular Ca^{2+} ($[Ca^{2+}]_i$) in trabeculae dissected from ventricles. We found that relaxation time and $[Ca^{2+}]_i$ decay (Tau) were prolonged during electrically stimulated twitch contractions in db/db mice, both of which were significantly ameliorated in the LIPUS-treated db/db mice, indicating that the LIPUS therapy also improves relaxation properties at tissue level. Functionally, exercise capacity was also improved in the LIPUS-treated db/db mice. Histologically, db/db mice displayed progressed cardiomyocyte hypertrophy and myocardial interstitial fibrosis, while those changes were significantly suppressed in the LIPUS-treated db/db mice. Mechanistically, western blot showed that the endothelial nitric oxide synthase (eNOS)-nitric oxide (NO)-cGMP-protein kinase G (PKG) pathway and Ca^{2+}-handling molecules were up-regulated in the LIPUS-treated heart.

Conclusions These results indicate that the LIPUS therapy ameliorates cardiac diastolic dysfunction in db/db mice through improvement of eNOS-NO-cGMP-PKG pathway and cardiomyocyte Ca^{2+}-handling system, suggesting its potential usefulness for the treatment of HFpEF patients.

*Corresponding author. Tel: +81 22 717 7152; fax: +81 22 717 7156, E-mail: shimo@cardio.med.tohoku.ac.jp

Graphical Abstract

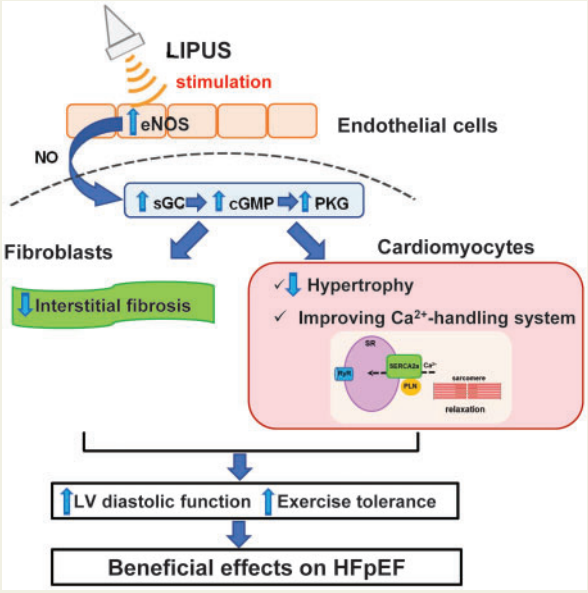

Keywords LIPUS • Diastolic function • Ca^{2+}-handling system • Non-invasive therapy • eNOS-NO-cGMP-PKG pathway

1. Introduction

Heart failure (HF) is a major cause of death in developed countries, and the number of patients has been increasing worldwide.[1,2] Especially, the prevalence of HF with preserved left ventricular (LV) ejection fraction (LVEF) (HFpEF) has been rapidly increasing worldwide, accounting for more than 50% of all HF patients.[1,2] For decades, effective treatments that improve HF with reduced LVEF have been developed. However, despite a number of large-scale clinical trials, no effective treatment to improve HFpEF is yet available. Indeed, HFpEF is a serious health problem worldwide.

Diastolic dysfunction is one of the most important pathophysiological factors of HFpEF.[3] HFpEF patients have elevated LV filling pressure and subsequent pulmonary hypertension, which is caused by abnormal LV diastolic function. In addition, epidemiological evidence suggests that diastolic dysfunction is present and progresses in severity before HF symptoms arise and that the severity of diastolic dysfunction is associated with an increased risk of symptomatic HF and mortality.[4] Thus, diastolic dysfunction plays an important role in the development and progress of HFpEF.

Recently, it has been proposed that vascular endothelial dysfunction and subsequent impairment of the endothelial nitric oxide synthase (eNOS)-nitric oxide (NO)-cGMP-protein kinase G (PKG) pathway underlie the pathophysiology of HFpEF, associated with comorbidities, such as hypertension, diabetes mellitus (DM), obesity, chronic kidney disease (CKD), and ageing.[5,6] Thus, the eNOS-NO-cGMP-PKG pathway could be a novel and promising therapeutic target for HFpEF.[5,7,8]

Low-intensity pulsed ultrasound (LIPUS) is a low power ultrasound with a certain pulse waveform.[9] In a series of studies, we demonstrated that LIPUS directly stimulates vascular endothelial cells and enhances the expression of eNOS and other angiogenic factors, improving myocardial ischaemia, and cardiac function in animal models of ischaemic heart disease and hypertensive heart disease.[10–12] We also have recently demonstrated that our LIPUS therapy is effective and safe in mouse models of dementia, where up-regulation of eNOS plays a central role.[13] Clinical trials are underway to evaluate the efficacy and safety of our LIPUS treatment in patients with severe angina and those with mild cognitive impairment in Japan. Based on these findings, we hypothesized that our LIPUS therapy is also effective for improving LV diastolic dysfunction. Thus, in the present study, we examined whether our LIPUS therapy also ameliorates diastolic dysfunction in a mouse model of HFpEF associated with Type 2 DM, and if so, to elucidate the mechanisms involved.

2. Methods

A detailed description of the methods is provided in the Supplementary material online.

2.1 Animal experiments

All animal experiments were performed along with the NIH guidelines (Guide for the care and use of laboratory animals) and were conducted in accordance with the protocols approved by the Institutional Committee for Use and Care of Laboratory Animals of Tohoku University (No. 2017-Idou-214). $Lepr^{db/db}$ mice (db/db mice), a leptin receptor-deficient model of obesity and Type 2 diabetes, and their non-diabetic lean heterozygous $Lepr^{db/+}$ littermates (db/+ mice) were purchased from Charles River Laboratories (BKS.Cg-Dock7$^{m+/+}$ $Lepr^{db}$/J).[14] The animals were randomly assigned to the groups with the LIPUS therapy (db/db-LIPUS group: $n = 42$ and db/+-LIPUS group: $n = 10$) or the groups with placebo procedure (db/db-control group: $n = 42$ and db/+-control group: $n = 17$). Some animals (db/db-control group:

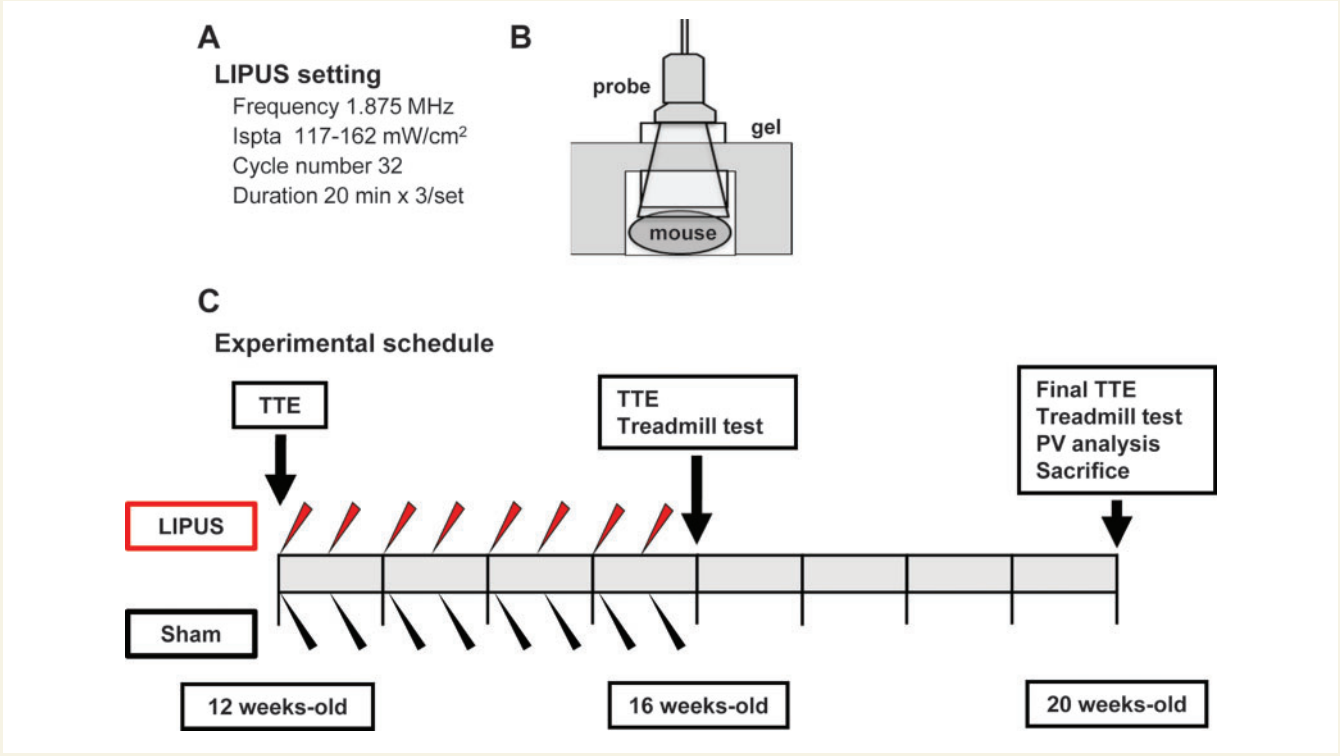

Figure 1 Study protocol. (*A*) The setting of the LIPUS therapy. (*B*) Schematic drawing showing the LIPUS application in a mouse heart. (*C*) Experimental protocol.

$n = 20$, db/db-LIPUS group: $n = 20$, db/+-control group: $n = 6$, db/+-LIPUS group: $n = 6$) were used for echocardiography examination, invasive haemodynamic analysis, exercise testing, blood tests, and histological analysis. Some animals were used for western blot analysis (db/db-control group: $n = 10$, db/db-LIPUS group: $n = 10$, db/+-control group: $n = 4$, db/+-LIPUS group: $n = 4$), measurement of force and intracellular Ca^{2+} in trabeculae (db/db-control group: $n = 5$, db/db-LIPUS group: $n = 5$), and Langendorff experiments (db/+-control group: $n = 7$, db/db-control group: $n = 7$, db/db-LIPUS group: $n = 7$). Every three to six mice were separated in the cages where the temperature (22°C) and humidity (60%) were kept stable, and they were fed with food and water supplied at *ad libitum*.

2.2 The LIPUS therapy

For the LIPUS therapy, a diagnostic ultrasound device (Prosound α10; HITACHI, Ltd., Tokyo, Japan) whose treatment conditions could be modified by software application was used.[11,12] The probe used for the treatment was a sector-type probe commercially available as a diagnostic device for humans. Based on our previous studies,[11,12] we performed the LIPUS therapy under the following conditions; frequency 1.875 MHz, pulse repetition frequency 4.90 kHz, number of cycles 32, voltage applied to each transducer element 17.67 volts (V), Ispta (spatial peak temporal average intensity) 117–162 mW/cm^2, and the power of the LIPUS was 0.25 W/cm^2 (*Figure 1A*).[11,12] The beam of therapeutic ultrasound was irradiated as sector shape and focused at 6 cm depth. For safety, to prevent the temperature rise of the ultrasound probe, the voltage applied to each transducer element was controlled to keep the level lower than the upper limit of acoustic output standards (<720 mW/cm^2) for diagnostic ultrasound devices (US Food and Drug Administration's Track 3 Limits). In order to irradiate the heart with stable sound field, LIPUS was applied to mice through an agar phantom gel (*Figure 1B*). LIPUS was applied to the heart through the chest wall under light anaesthesia with inhaled isoflurane (0.5–1.0%). The animals in the LIPUS group were subjected to the LIPUS therapy two times a week for 4 weeks from 12- to 16-weeks-old (*Figure 1C*). The animals in the control group underwent the same procedures including anaesthesia but without the LIPUS therapy (*Figure 1C*).

2.3 Transthoracic echocardiography

Transthoracic echocardiography was performed under light anaesthesia with inhaled isoflurane (0.4–1.5%) at 12, 16, and 20-weeks-old, using Vevo 2100 (Visual Sonics, Ontario, Canada) as previously reported.[15] Heart rate during echocardiographic study was maintained in the range of 500∼600 b.p.m. for M-mode and B-mode, respectively and 450∼550 b.p.m. for Doppler studies.[15]

2.4 Invasive pressure–volume analysis

Invasive haemodynamic measurements were performed in anaesthetized mice with inhaled isoflurane (0.4–1.5%) and mechanical ventilation at 20-weeks-old. After thoracotomy, a 4-electrode pressure conductance catheter (1.4 F, SPR-839, Millar Instruments, Houston, TX, USA) was inserted into the LV through the apex. After stabilization, steady-state measurements were recorded. Subsequently, LV preload was decreased by occlusion of the inferior vena cava for 5–10 s to obtain the slope of the LV end-diastolic pressure–volume relationship (EDPVR) (PowerLab/4SP, AD Instruments, Lab Chart 7 Pro Software, Castle Hill, Australia).[14] All data were analysed using the PowerLab data acquisition system (AD Instruments) and averaged over 10 sequential beats.

2.5 Blood pressure measurement

Blood pressure was measured at 12-, 16-, and 20-weeks-old with the tail-cuff system (Muromachi Kikai Co, Ltd, MK-2000ST NP-NIBP Monitor, Tokyo, Japan) without anaesthesia.

2.6 Exercise testing

Exercise capacity of mice was examined using a 6-lane rodent treadmill system (MK-680C, Muromachi Kikai, Japan) at 12-, 16-, and 20-weeks-old. After 10 min of acclimatization running at a low speed (1 m/min), exercise testing was performed by progressively increasing speed (speed steps of 1 m/min every 2 min). Maximal speed and running distance were determined when the mouse left the treadmill and remained on a shock pad for 5 s. Exercise capacity was expressed as work load in Jules (J), calculated by multiply running distance by body weight. All animals were given water and standard rodent feed ad libitum pre- and post-exercise.

2.7 Measurement of force and intracellular Ca^{2+} in mouse trabeculae

After the mice were adequately anaesthetized with intraperitoneal injection of butorphanol tartrate (5.0 mg/kg), midazolam (4.0 mg/kg), and medetomidine chloride (0.3 mg/kg),[16] according to the Guide for the care and use of laboratory animals, the mouse heart was excised, coronary arteries were immediately perfused via the aorta with a HEPES buffered solution with 15 mmol/L KCl. The trabeculae were dissected from the endocardial region of the right ventricle and mounted on an inverted microscope (Nikon, Japan) between a force transducer and a micromanipulator in a bath superfused with HEPES solution containing 5 mM KCl as described previously.[17,18] Force was measured using a silicon strain gauge (model AE-801, SenSoNor, Horten, Norway). Intracellular Ca^{2+} level was measured using microinjected fura-2 and a photomultiplier tube (PMT; E1341 with a C1556 socket, Hamamatsu, Japan).[17–19] The trabeculae were electrically stimulated with parallel platinum electrodes at 0.5 Hz (22°C, extracellular Ca^{2+} = 2.0 and 4.0 mM).[18,19]

2.8 Biochemical analysis

Serum levels of blood glucose and insulin were measured using a glucometer and an insulin ELISA kit [Mouse Insulin ELISA kit (#10-1247-01), Mercodia AB, Uppsala, Sweden], respectively. Serum B-type natriuretic peptide (BNP) levels were measured using a BNP ELIZA kit [ELISA Kit for Brain Natriuretic Peptide (CEA541Ca), Cloud-Clone Corp., TX, USA]. Western blot analysis was performed by standard methods.

2.9 Histological analysis

Excised hearts were fixed with 4% formalin for histological and immunohistochemical examinations. The tissue specimens were embedded in paraffin and sliced at 3-μm in thickness. The sections were stained by haematoxylin & eosin (H&E) and Masson-trichrome (MT); the latter was used to assess LV myocardial fibrosis. CD31 immunostaining was used to assess myocardial capillary density. The hypoxic regions in the heart were evaluated by hypoxyprobe-1 kit (HP1-100Kit, Hypoxyprobe Inc., MA, USA), according to the manufacturer's instructions. Semi-quantitative analysis regarding the extent of hypoxyprobe was evaluated for each image by using the following scale; 0 = none, 1 = slight, 2 = moderate, and 3 = high, as previously described.[12] In all analysis, three sections were assessed per animals.

2.10 Indirect NO measurement

We performed indirect measurement of NO, using the OxiSelect Nitrite Assay Kit (Cell Biolabs, San Diego, CA, USA) based on the conversion of nitrate to nitrite by nitrate reductase followed by quantification of nitrate after the Griess reaction. NOx (NO_2 + NO_3) level was measured according to the Product Manual.

2.11 Langendorff experiments

Langendorff experiments were performed as previously described.[20–22] Mice were pretreated intraperitoneally with heparin (500 units) and 10 min later, they were sacrificed with intraperitoneal injection of pentobarbital sodium (50 mg/kg). The hearts were excised and placed into ice-cold Krebs-Henseleit buffer (KHB) to be arrested. After all extra-aortic tissues were removed, the ascending aorta was cannulated with a 21-guage blunted needle and tied up with a thread. Then, the heart was retrogradely perfused at a constant flow of 2.0 mL/min by the Langendorff apparatus (Model IPH-W2, Primetech Corporation, Tokyo, Japan) with warmed KHB bubbled with 95% O_2 and 5% CO_2. After a 10-min stabilization period, the heart was paced at 400 b.p.m. and then perfused at a constant pressure of 80 mmHg. Coronary flow was continuously measured with a flowmeter using an ultrasonic flow probe (FLSC-01, Primetech Corporation, Tokyo, Japan) and was analysed by a computer-based analysis system in LabChart 7.0 software. Bradykinin (BK, 10^{-6} mol/L) and sodium nitroprusside (SNP, 10^{-5} mol/L) were used to evaluate endothelium-dependent and -independent vasodilator responses, respectively. Coronary flow rate was corrected by heart weight. Baseline coronary flow was defined as coronary flow rate before administration of vasodilator agonists. Increases in coronary flow were calculated as the difference between maximum coronary flow in response to vasodilators and baseline coronary flow (Supplementary material online, *Figure S8A*).

2.12 Statistical analysis

Results are shown as mean ± standard deviation for all experiments. Differences between two groups were analysed using an unpaired two-tailed Student's *t*-test or Wilcoxon rank sum test as appropriate. Data from multiple groups were analysed using analysis of variance followed by Tukey's multiple comparison for normally distributed samples with equal variances. The normality of the distributions was confirmed by the Shapiro's normality test, and the equality of the variances was tested by the Bartlett test. For comparisons of the groups with skewed distributions and unequal variances, we applied non-parametric multiple contrast test procedure proposed by previous reports[23] (GraphPad Prism Software Inc., San Diego, CA, USA and R version 3.6.3). Differences with a *P*-value <0.05 were considered to be statistically significant.

3. Results

3.1 db/db mice

Body weight was greater in db/db mice than in db/+ mice by more than two-fold, whereas no significant difference was noted between db/db-control and db/db-LIPUS mice (Supplementary material online, *Figures S1A* and *S3A*). During the experiment, systolic blood pressure (BP) and diastolic BP tended to elevate in both db/db-control and db/db-LIPUS mice compared with db/+ mice. However, there was no statistical difference in systolic or diastolic BP between db/db-control and db/db-LIPUS mice (Supplementary material online, *Figure S1B* and *C*).

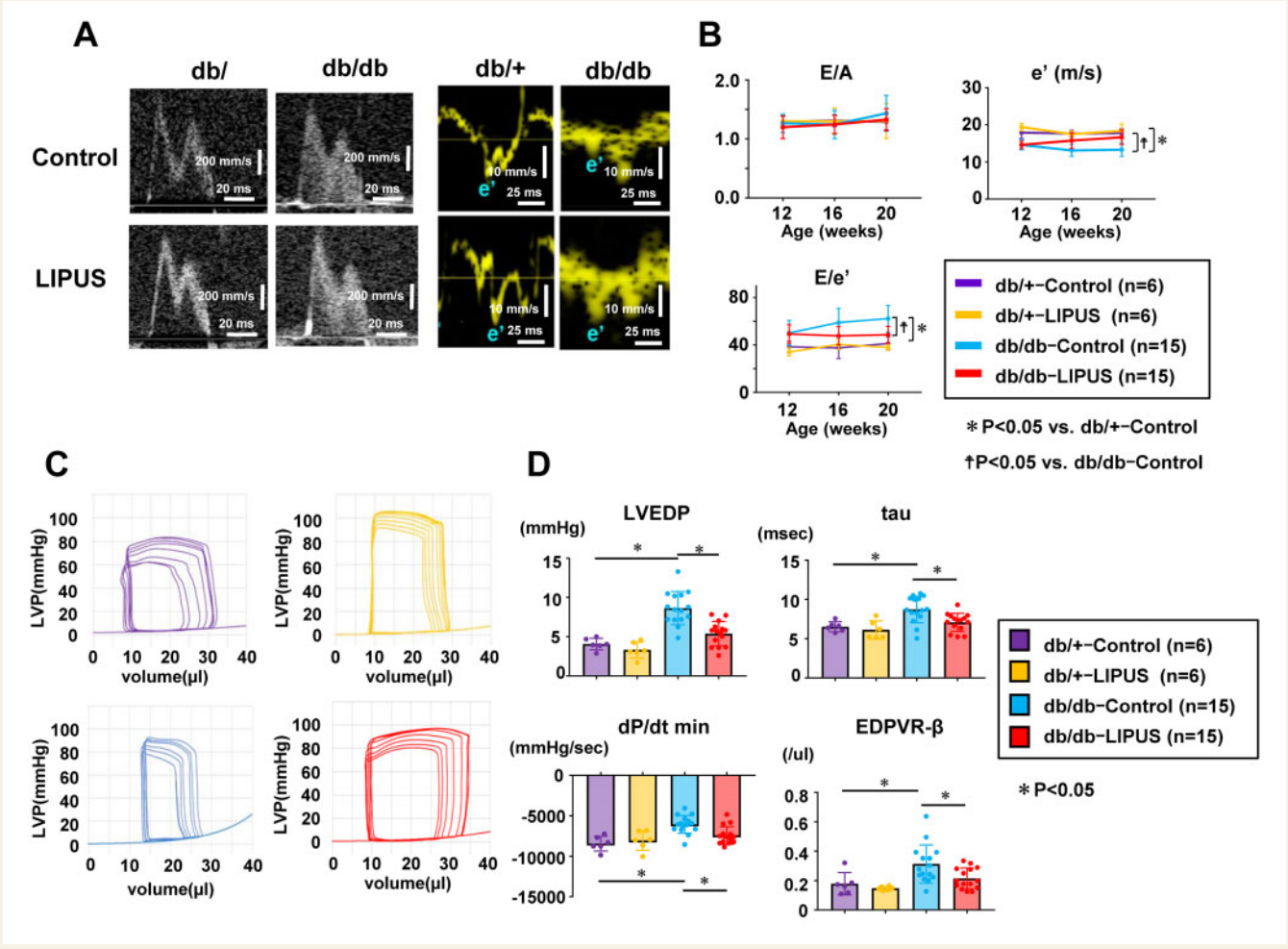

Figure 2 LIPUS therapy significantly improves LV diastolic dysfunction in db/db mice. (*A*) Representative echocardiographic mitral inflow pattern with Doppler imaging (scale bars, 25 ms and 10 mm/s) and septal mitral annular velocity with tissue Doppler imaging (scale bars, 20 ms and 200 mm/s) at 20-weeks-old. (*B*) Graphs showing the time-course of *E/A* ratio, mitral *e′*, and *E/e′* ratio. (*C*) Representative LV pressure–volume loops with vena cava occlusion at 20-weeks-old. (db/+-control: $n = 6$, db/+-LIPUS: $n = 6$, db/db-control: $n = 15$, db/db-LIPUS: $n = 15$). (*D*) Graphs showing end-diastolic pressure (EDP), time constant of LV pressure decay (tau), d*P*/d*t* min, and slope of the end-diastolic pressure–volume relationship (EDPVR) (db/+-control: $n = 6$, db/+-LIPUS: $n = 6$, db/db-control: $n = 15$, db/db-LIPUS: $n = 15$). Results are expressed as mean ± SD. Comparisons of parameters were performed with ANOVA followed by Tukey's test for multiple comparisons, or non-parametric multiple comparison test. Differences with a *P*-value <0.05 were considered to be statistically significant.

3.2 Lipus therapy ameliorates cardiac diastolic dysfunction in db/db mice

Echocardiographic study showed that, in both db/db-control and db/db-LIPUS mice, LV wall was slightly thicker than in db/+-control mice, although no difference was noted between the two db/db mouse groups (Supplementary material online, *Figure S2B* and *C*). Also, there was no significant difference in LV end-diastolic dimension (LVDd) among the four groups (Supplementary material online, *Figure S2D*). Regarding of calculated LV mass, there was a trend of increase, but not significant, in db/db-control group compared with db/+-control mice. On the other hand, this change was tend to be suppressed in db/db-LIPUS mice compared with db/db-control mice (Supplementary material online, *Figure S2E*). Left atrial dimension was significantly larger in both db/db mice than in db/+-control mice, but no difference was noted between db/db-control and db/db-LIPUS mice (Supplementary material online, *Figure S2F*). Regarding the parameters of cardiac systolic functions, there was no significant difference in LVEF or LV fractional shortening among the four groups, suggesting that cardiac systolic function was preserved in db/db mice (Supplementary material online, *Figure* 2G *and H*). In contrast, db/db-control mice showed lower *e′* and higher *E/e′* than db/+-control mice, indicating impaired cardiac diastolic function. Importantly, *e′* and *E/e′* were significantly ameliorated in db/db-LIPUS mice (*Figure* 2A *and B*). For further detailed examinations of cardiac functions, we also performed invasive haemodynamic evaluations. Consistent with the results of echocardiography, db/db-control mice, when compared with db/+ mice, showed diastolic dysfunction characterized by elevated LV end-diastolic pressure (LVEDP), prolonged tau, reduced negative d*P*/d*t*, and increased slope of EDPVR (*Figure* 2C *and D*). Despite marked diastolic dysfunction in db/db-control mice, conventional systolic function parameters, such as stroke work, cardiac output, and positive d*P*/d*t*, were comparable among the four groups (Supplementary material online, *Figure 4A, B*, and *F*). Importantly, the LIPUS therapy markedly improved

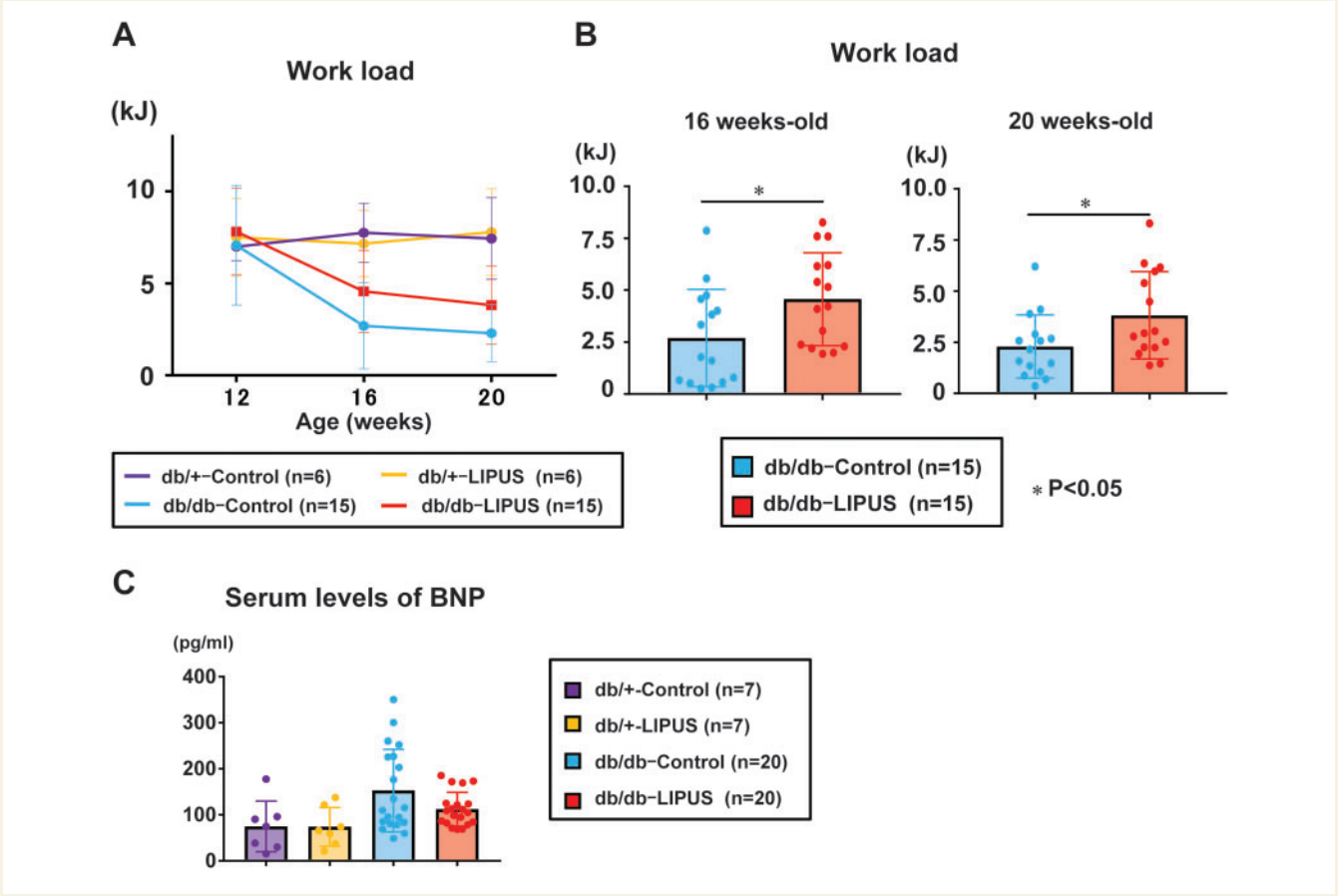

Figure 3 LIPUS improves exercise tolerance and decreases serum BNP levels in db/db mice. (*A*) Graphs showing the time-course of exercise capacity (work load) measured by treadmill test from 12- to 20-weeks-old (db/+-control, $n = 6$; db/+-LIPU, $n = 6$; db/db-control, $n = 15$; db/db-LIPUS, $n = 15$). (*B*) In the LIPUS group, work load was fairly preserved compared with the control group at 16- and 20-weeks-old (db/db-control, $n = 15$; db/db-LIPUS, $n = 15$). (*C*) Graph showing the serum levels of BNP at 20-weeks-old (db/+-control: $n = 7$, db/+-LIPUS: $n = 7$, db/db-control: $n = 20$, db/db-LIPUS: $n = 20$). Results are expressed as mean ± SD. Comparisons of parameters were performed with unpaired Student's *t*-test, or Wilcoxon rank sum test. Differences with a *P*-value <0.05 were considered to be statistically significant.

diastolic function parameters, such as EDP, tau, negative d*P*/dt, and the slope of EDPVR (*Figure* 2C *and D*).

3.3 Lipus therapy improves exercise tolerance and decreases serum levels of BNP in db/db mice

Although the treadmill running distance was significantly shorter in db/db mice than in db/+ mice, work load was not significantly different among four groups at 12-weeks-old (*Figure 3A* and Supplementary material online, *Figure S5A*). Throughout the experimental period, work load remained unchanged in db/+ mice (*Figure 3A*). However, work load was reduced with ageing in db/db mice, which suggested reduced exercise capacity (*Figure 3A*). At 16- and 20-weeks-old, the distance and work load was significantly larger in db/db-LIPUS mice than in db/db-control mice, indicating the improvement of exercise capacity (*Figure 3B*). In addition, regarding of serum BNP levels, db/db mice tended to increase than db/+ mice (*Figure 3C*). On the other hand, serum BNP levels were significantly lower in in db/db-LIPUS group (111.9 ± 36.8 pg/mL) than db/db-control mice (152.4 ± 89.7) at 20-weeks-old in the comparison with unpaired Student's *t*-test ($P < 0.05$).

3.4 Lipus therapy suppresses myocardial hypertrophy and interstitial fibrosis

Histologically, in db/db mice, heart weight (HW), and HW/tibial length (TL) ratio were significantly greater compared with db/+-control mice. In db/db-LIPUS mice, HW and HW/TL ratio significantly decreased compared with db/db-control mice (Supplementary material online, *Figure S3B* and *C*). Regarding glucose tolerance, db/db mice showed hyperglycaemia and hyperinsulinaemia, but there was no difference between db/db-control and db/db-LIPUS mice (Supplementary material online, *Figure S3E* and *F*). H&E staining showed that myocardial cross-sectional area (CSA) was significantly increased in db/db-control mice compared with db/+-control mice (*Figure* 4A *and B*). Importantly, in db/db-LIPUS mice, CSA significantly decreased compared with db/db-control mice (*Figure* 4A *and B*), indicating that the LIPUS therapy suppressed myocardial hypertrophy in those mice. Masson trichrome staining showed that myocardial interstitial fibrosis was advanced in db/db-control mice compared with db/+-control mice (*Figure* 4A *and C*) and was also slightly but significantly suppressed in db/db-LIPUS mice compared with db/db-control mice, suggesting that the LIPUS therapy suppressed the fibrotic remodelling in those mice (*Figure* 4A *and C*).

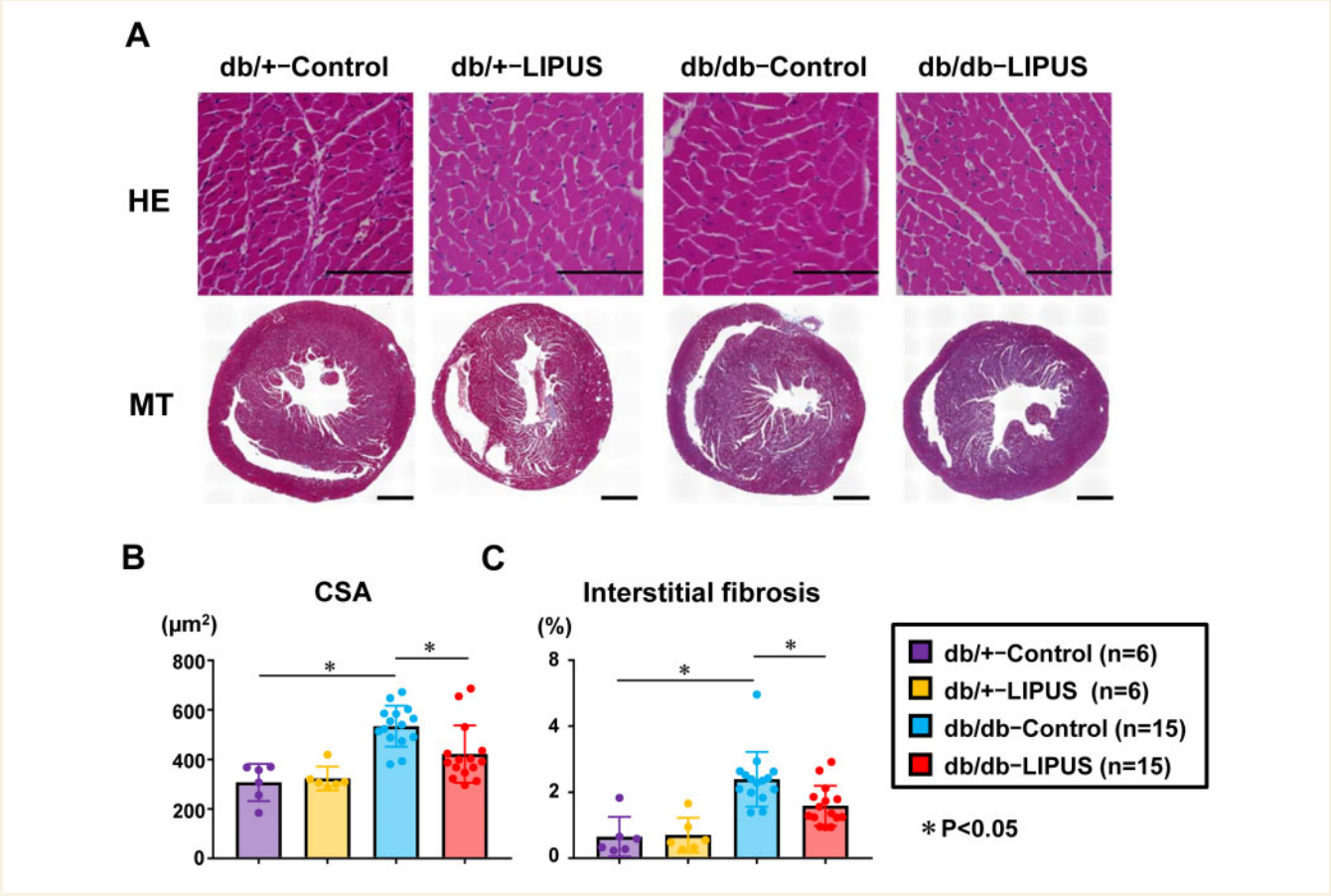

Figure 4 LIPUS therapy attenuates cardiomyocyte hypertrophy and interstitial fibrosis in db/db mice. (*A*) Representative images of myocardial tissues stained with haematoxylin–eosin (H&E, upper, scale bars, 100 μm) and Masson-trichrome (MT, lower, scale bars, 1 mm) at 20-weeks-old. (*B*) Quantitative analysis of cross-sectional area (H&E staining). (*C*) Quantitative analysis of myocardial fibrosis area (MT staining) (db/+-control: $n = 6$, db/+-LIPUS: $n = 6$, db/db-control: $n = 15$, db/db-LIPUS: $n = 15$). Results are expressed as mean ± SD. Comparisons of parameters were performed with one-way ANOVA followed by Tukey's multiple comparisons, or non-parametric multiple comparison test. Differences with a *P*-value <0.05 were considered to be statistically significant.

3.5 Effects of the LIPUS therapy on capillary density and coronary blood flow

Recently, coronary microcirculatory dysfunction is recognized to play an important role in the pathophysiology of HFpEF.[7,24] It has been proposed that microvascular rarefaction and microvascular endothelial dysfunction could impair oxygen supply to the myocardium and promote myocardial hypertrophy and fibrosis, resulting in cardiac diastolic dysfunction.[25] Thus, we examined whether cardiac diastolic dysfunction in db/db mice is associated with myocardial ischaemia and/or with alternation in coronary microcirculation, and if so, whether the LIPUS therapy could improve it. Histological analysis showed that there was no significant difference in capillary density among the four groups (Supplementary material online, *Figure S7A* and *B*). We further examined the extent of myocardial ischaemia by hypoxyprobe staining and found no significant difference among the four groups (Supplementary material online, *Figure S7A* and *C*). These results indicated that db/db mice did not display myocardial microvascular rarefaction or myocardial ischaemia and that LIPUS did not affect them.

In addition, in order to examine the effects of the LIPUS therapy on coronary microcirculation, we performed Langendorff experiments, in which we measured coronary blood flow in response to endothelium-dependent and -independent vasodilators. At baseline, there was no significant difference in coronary blood flow between db/+ mice and db/db mice and LIPUS did not have significant effect on coronary blood flow in db/db mice (Supplementary material online, *Figure S8B*). However, endothelium-dependent increase in coronary flow in response to BK tended to be decreased in db/db-control mice compared with db/+ mice, which was ameliorated in db/db-LIPUS group (Supplementary material online, *Figure S8B*). In contrast, endothelium-independent increase in coronary flow in response to SNP was comparable among the three groups (Supplementary material online, *Figure S8C*).

3.6 Lipus therapy improves relaxation properties of isolated myocardial tissue in db/db mice

It was previously reported that Ca^{2+} handling system is impaired in diabetic heart with resultant impairment of relaxation capacities at both myocardial tissue and cardiomyocyte levels.[26] To evaluate the effects of LIPUS on myocardial relaxation capacities and Ca^{2+} flux at a tissue level, we examined force and intracellular Ca^{2+} concentration ($[Ca^{2+}]_i$) in the

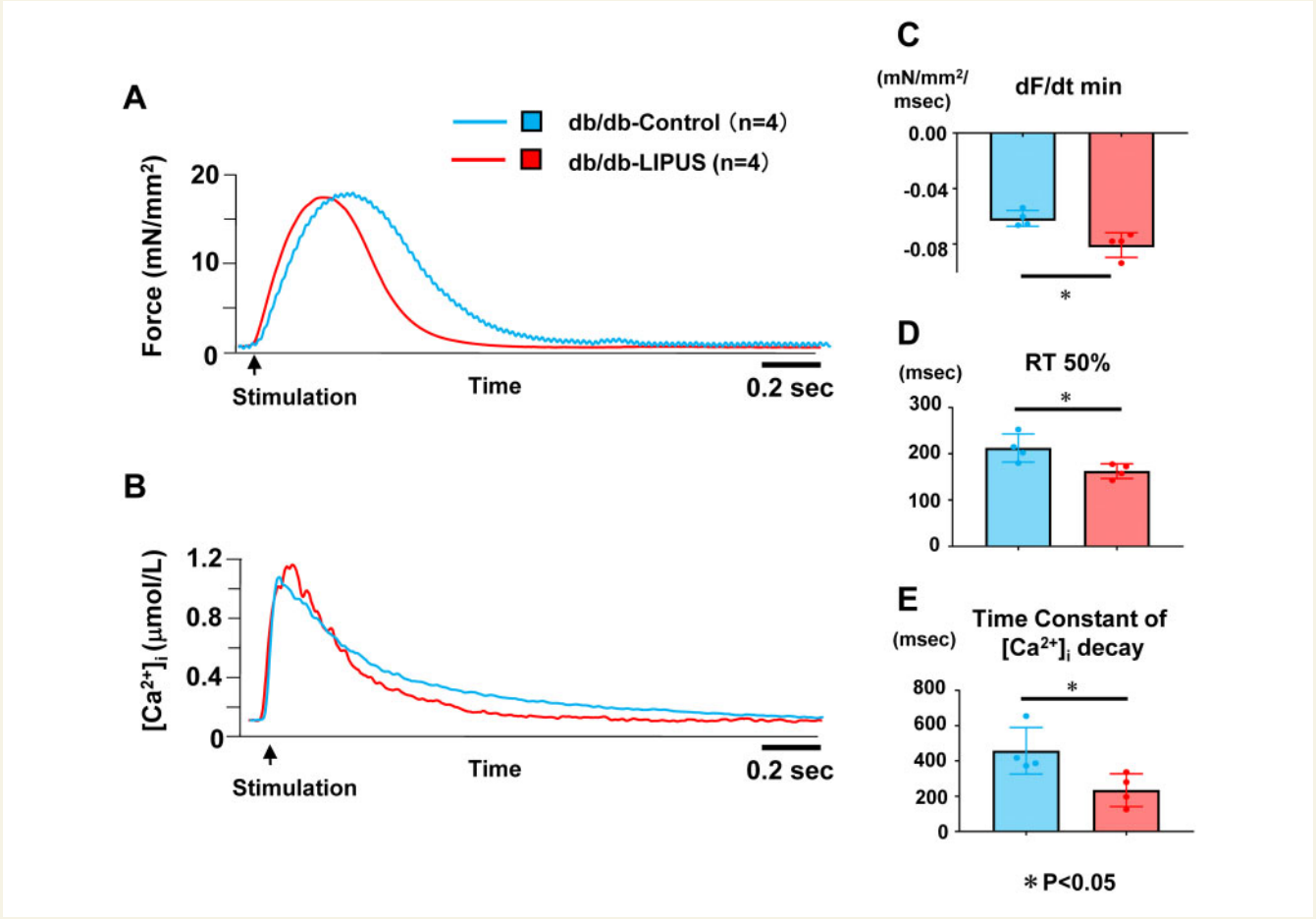

Figure 5 LIPUS therapy improves relaxation properties of isolated myocardial tissue *in vitro*. (*A* and *B*) Representative tracings of force and intracellular Ca^{2+} ($[Ca^{2+}]_i$) by 0.5 Hz electrical stimulation (22°C, extracellular Ca^{2+} = 4.0 mmol/L) in the trabeculae dissected from the right ventricles at 20-weeks-old. (*C–E*) Graph showing relaxation rate (d*F*/d*t* min), relaxation time to 50% relaxation (RT50%), and time constant of $[Ca^{2+}]_i$ decay (n = 4) trabeculae per group (one trabeculae per one mouse). Results are expressed as mean ± SD. Comparisons of parameters were performed with unpaired Student's *t*-test, or Wilcoxon rank sum test. Differences with a *P*-value <0.05 were considered to be statistically significant.

trabeculae dissected from the right ventricle during electrical stimulation. There was no difference in developed force, peak $[Ca^{2+}]$i, or positive peak derivative forces (d*F*/d*t* max) between db/db-control and db/db-LIPUS mice, indicating that LIPUS had no effect on myocardial contractility (Supplementary material online, *Figure S6A–C*). In contrast, negative peak derivative force (d*F*/d*t* min) and relaxation time to 50% relaxation (RT50%) were significantly increased in db/db-LIPUS mice compared with db/db-control mice group, indicating that the LIPUS therapy improved relaxation ability of diabetic myocardial tissue (*Figure 6C and D*). Consistently, the trabeculae from db/db-LIPUS mice showed reduced time constant of $[Ca^{2+}]_i$ decay compared with db/db-control mice (*Figure 6E*), whereas there was no significant difference in diastolic $[Ca^{2+}]_i$ (Supplementary material online, *Figure S6E*). These results indicate that the LIPUS therapy ameliorates myocardial relaxation property but not contractility.

3.7 Effects of the LIPUS therapy on Ca^{2+}-handling proteins

In order to elucidate the molecular mechanisms of the beneficial effects of LIPUS on relaxation properties and Ca^{2+} cycling at myocardial tissue level, we examined the protein expressions and activity of Ca^{2+}-handling molecules in the myocardium, including sarcoplasmic reticulum Ca^{2+}-ATPase (SERCA2a) and phospholamban (PLN). The expression level of phosphorylated PLN at Ser16, but not that at Thr17, was significantly lower in db/db-control than in db/+-control mice, and the phosphorylation level tended to be restored in db/db-LIPUS mice (*Figure 6A–C*). In contrast, there was no difference in the expression of PLN among the four groups (*Figure 6D*). Additionally, the expression of SERCA2a was significantly up-regulated in db/db-LIPUS mice compared with db/db-control mice (*Figure 6E*). The ratio of SERCA/PLN was also significantly increased in db/db-LIPUS mice compared with db/db-control mice (*Figure 6F*).

3.8 Effects of the LIPUS therapy on the expression and phosphorylation of sarcomeric proteins

Recent studies have shown that the expression and function of sarcomeric proteins are closely related to myocardial diastolic function.[27] In order to examine the effects of the LIPUS therapy on sarcomeric proteins such as TnI and MyBP-C, we examined the expression and

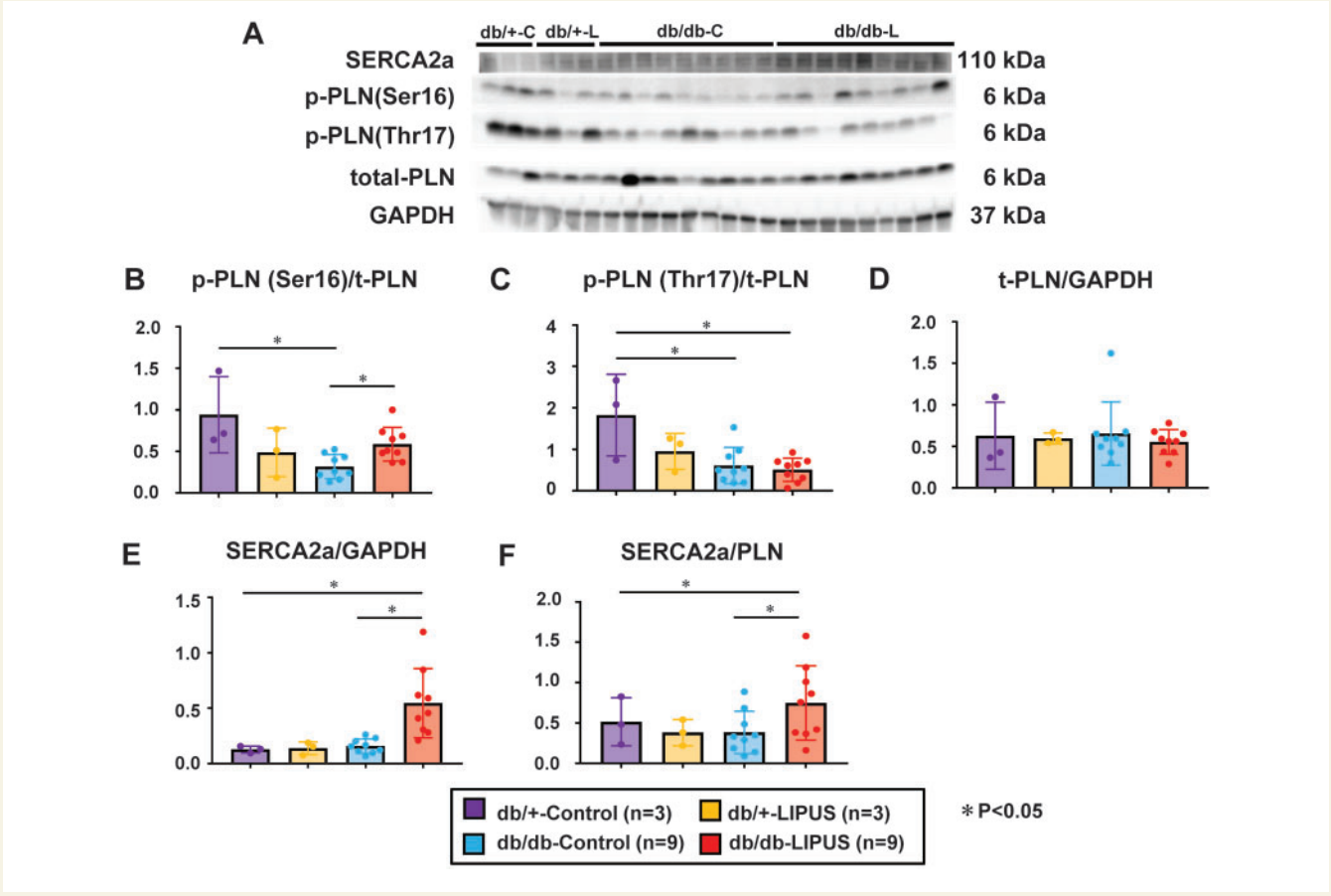

Figure 6 LIPUS therapy improves the expressions of Ca^{2+} handling-related proteins. (*A–E*) Representative western blot and quantification of phospholamban (PLN) phosphorylation (Ser16/Thr17), total PLN, SERCA2a, and SERCA2a/PLN ratio in mice (db/+-control: $n = 3$, db/+-LIPUS: $n = 3$, db/db-control: $n = 9$, db/db-LIPUS: $n = 9$). Results are expressed as mean ± SD. Comparisons of parameters were performed with one-way ANOVA followed by Tukey's multiple comparisons, or non-parametric multiple comparison test. Differences with a *P*-value <0.05 were considered to be statistically significant.

phosphorylation of those proteins. There was no significant difference in the expression of TnI nor MyBP-C among the four groups (Supplementary material online, *Figure S10B* and *D*). Regarding the phosphorylation, there was no difference in the expression level of phosphorylated TnI among the four groups (Supplementary material online, *Figure S10C*). In addition, although the expression level of phosphorylated MyBP-C tended to increase in db/db mice compared with db/+ mice, there was no significant difference among the four groups (Supplementary material online, *Figure S10D*).

3.9 Lipus therapy up-regulates the eNOS-NO-cGMP-PKG signalling pathway

To further elucidate the underlying molecular mechanisms of the beneficial effects of the LIPUS therapy on cardiac diastolic functions, we performed Western blotting for several proteins. The LIPUS therapy had no effects on the eNOS-NO-cGMP-PKG signalling pathway in non-diabetic mice (*Figure 7A–F*). Importantly, the LIPUS therapy significantly increased myocardial level of phosphorylated eNOS in db/db-LIPUS mice than in db/db-control mice (*Figure 7C*). Furthermore, the LIPUS therapy significantly up-regulated the expression of the downstream molecules, such as soluble guanylate cyclase (sGC) and PKG I, in db/db mice (*Figure 7D–F*). In addition, we performed indirect measurement of NO by measuring NOx (NO_2+NO_3) level in the myocardium. Although db/db mice showed lower levels of NOx level compared with db/+ mice, there was no significant difference between db/db-LIPUS mice and db/db-control mice (Supplementary material online, *Figure S9*).

4. Discussion

The novel findings of the present study were that the LIPUS therapy markedly improved cardiac diastolic dysfunction and exercise tolerance without any adverse effects in obese db/db mice with Type 2 DM, for which enhancement of the eNOS-NO-cGMP-PKG signalling pathway and improvement of myocardial Ca^{2+}-handling proteins are involved (Graphical abstract). To the best of our knowledge, this is the first report demonstrating that the LIPUS therapy is effective and safe to improve cardiac diastolic function in a mouse model of DM/obesity-related HFpEF. The present results suggest that the LIPUS therapy is a promising, novel, and non-invasive therapy for cardiac diastolic dysfunction in HFpEF patients.

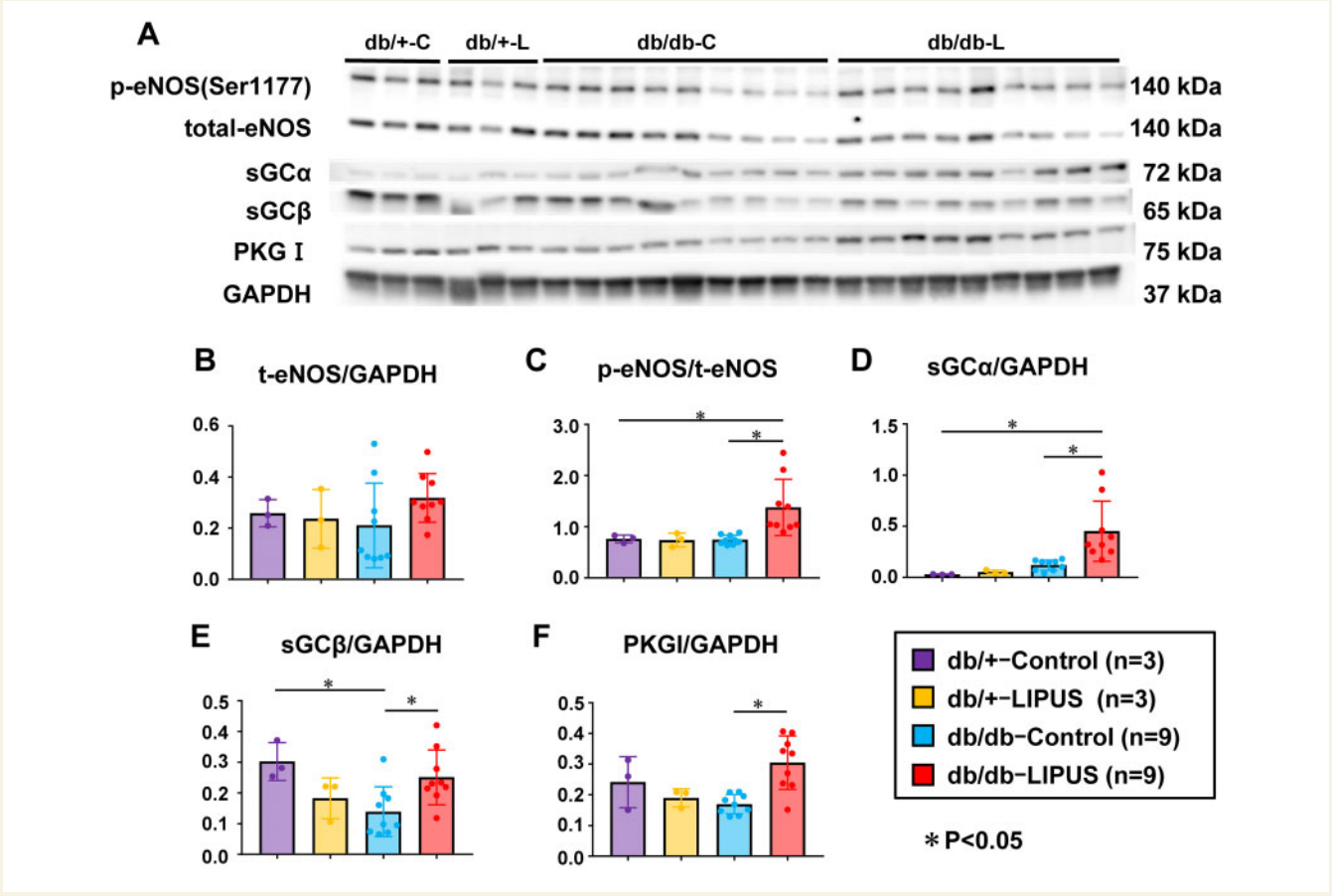

Figure 7 LIPUS therapy activates the eNOS-NO-cGMP-PKG signalling pathway. (*A–F*) Representative western blot and quantification of eNOS, phosphorylaed eNOS at Ser1177, soluble guanylated cyclase α (sGCα), sGCβ, and protein kinase G I in the mouse heart at 16-weeks-old. (db/+-control: n = 3, db/+-LIPUS: n = 3, db/db-control: n = 9, db/db-LIPUS: n = 9) Results are expressed as mean ± SD. Comparisons of parameters were performed with one-way ANOVA followed by Tukey's multiple comparisons, or non-parametric multiple comparison test. Differences with a P-value <0.05 were considered to be statistically significant.

4.1 Cardiac diastolic dysfunction in db/db mice

HFpEF is closely associated with LV diastolic dysfunction, which can be caused by increased LV stiffness due to hypertrophy and interstitial fibrosis and abnormal LV relaxation due to impaired calcium cycling.[3] HFpEF patients often have various comorbidities with endothelial dysfunction, where DM is one of the most frequent comorbidities.[28] Indeed, it has been reported that about 45% of HFpEF patients have DM, with highest prevalence noted in those with new-onset HFpEF.[2,29] It also has been reported that DM itself has a close correlation with cardiac diastolic dysfunction in diabetic patients.[30] In addition, DM is associated with adverse cardiovascular outcomes in HFpEF patients.[31] Thus, the pathophysiology of DM-associated HFpEF remains to be fully elucidated for development of a novel therapeutic strategy.

Metabolic stress due to DM and obesity is thought to be one of the major mechanisms underlying HFpEF pathophysiology.[6] db/db mice are an established animal model of obese-related Type 2 DM due to leptin receptor mutations.[32] They exhibit LV diastolic dysfunction accompanied by LV hypertrophy and fibrosis and preserved LV systolic function.[14,33] Since such features are also noted in patients with HFpEF and diabetic patients, db/db mice are widely used as a useful animal model of HFpEF.[32] In the present study with db/db mice, we also observed the typical phenotypes of cardiac diastolic dysfunction, including significant increase in LV stiffness and prolonged relaxation time in pressure–volume analysis, accompanied by morphological changes, such as myocardial hypertrophy and interstitial fibrosis, while cardiac systolic performance was preserved. In addition, we observed a reduced exercise tolerance in db/db mice, which is closely related to dyspnoea on exertion, the cardinal HFpEF symptom.[34]

4.2 Lipus therapy improved cardiac diastolic function and exercise capacity

In the present study, the LIPUS therapy ameliorated cardiac diastolic dysfunction as confirmed by echocardiography and invasive hemodynamic evaluation. Furthermore, at tissue level, we were able to demonstrate that LIPUS improved myocardial relaxation property. Such improvement of LV diastolic performance would contribute to decreases in LV filling pressure and serum BNP levels without decrease in systemic blood pressure.

More importantly, we showed that the improvement of cardiac function as described above has led to the improvement of exercise tolerance. Patients with HFpEF are characterized by reduced 'reserve

capacity'.[3,34] Indeed, although they are often asymptomatic at rest, under some stress conditions (e.g. exercise), LV filling pressure and pulmonary venous pressure increase, leading to HF symptoms (e.g. shortness of breath). Thus, the evaluation of exercise capacity is important in the evaluation of HFpEF patients.[34] In the present study, the LIPUS therapy improved exercise tolerance of db/db mice, indicating its potential usefulness for HFpEF patients.

4.3 Mechanism of the beneficial effects of LIPUS therapy on cardiac diastolic function

We have previously demonstrated that LIPUS stimulates endothelial cells and enhances eNOS activity.[11–13] In endothelial cells, eNOS localizes in the caveolae of the endothelial membrane, which is known to be flow-sensing organelles and converts mechanical stimuli (e.g. blood flow-induced shear stress) into chemical signals.[11,35] Cyclic strain induced by ultrasonic pulse waves is also sensed by the caveolae, leading to eNOS activation.[11,36] Indeed, in the present study, we demonstrated that the LIPUS therapy activates eNOS and up-regulates downstream molecules such as sGC and PKG, indicating that LIPUS activates the eNOS-NO-cGMP-PKG pathway.

Cardiac diastolic function is determined by myocardial stiffness associated with myocardial hypertrophy and fibrosis and relaxation ability associated with myocardial Ca^{2+} flux. The eNOS-NO-cGMP-PKG pathway is closely related to myocardial stiffness. It was shown that modulation of the sGC-PKG pathway with sildenafil was effective to suppress myocardial remodelling through inhibition of myocardial hypertrophy and interstitial fibrosis *in vivo*.[37] Hamdani *et al.* reported that pharmacological up-regulation of the myocardial cGMP-PKG pathway attenuates myocardial hypertrophy and fibrosis, leading to significant improvement of cardiac diastolic dysfunction in a mouse model of DM-related HFpEF.[14] In addition, other previous reports showed that the enhancement of the eNOS-NO-cGMP-PKG pathway suppressed myocardial hypertrophy and interstitial fibrosis.[14,38,39] In the present study, the LIPUS therapy suppressed myocardial hypertrophy and interstitial fibrosis, and subsequently improved LV stiffness in the hearts of db/db mice through the enhancement of the eNOS-NO-cGMP-PKG pathway.

On the other hand, the eNOS-NO-cGMP-PKG pathway is closely related to myocardial relaxation ability.[40] Active relaxation is determined by energy-dependent removal of Ca^{2+} from the cytosol, and the rate of cytosolic Ca^{2+} clearance during diastolic phase determines the pattern of muscle relaxation.[41] This process of dynamic change in cytosolic Ca^{2+} is known to be regulated by Ca^{2+} handling-related proteins, such as SERCA2a and PLN.[41] Several studies using rodent models of HF demonstrated that restoring the eNOS-NO-cGMP-PKG pathway could improve myocardial Ca^{2+} handling and its molecular modulation with resultant therapeutic effects on cardiac function.[40] It also has been reported that cardiomyocyte-specific PKG-KO mice showed attenuated expression of SERCA2a and PLN and diminished PLN phosphorylation at Ser16, the target site for PKG activation.[42] In the present study, we demonstrated that the LIPUS therapy improves LV active relaxation through ameliorating the Ca^{2+} clearance ability and the relaxation rate of myocardial tissue. Consistently, the expression and activation of Ca^{2+}-handling molecules, such as SERCA2a and PLN, were significantly enhanced along with the activation of the eNOS-NO-cGMP-PKG pathway. In contrast, although sarcomeric proteins (e.g. TnI and MyBP-C) are closely related to myocardial relaxation properties,[27] the LIPUS therapy had no effect on their expression or phosphorylation. The present study provides the first evidence that the LIPUS therapy improves Ca^{2+} handling system and myocardial relaxation property.

4.4 Effects of LIPUS on angiogenesis and coronary microcrocirculation in db/db mice

We previously demonstrated in several HF animal models that the cardioprotective effects of the LIPUS therapy are mediated in part through enhanced angiogenesis.[10–12] However, in the present study, no obvious angiogenic effects were noted. This is probably because capillary density was not reduced and there was no myocardial ischaemia in db/db heart (Supplementary material online, *Figure S7*). This finding is consistent with our previous finding that the LIPUS therapy promotes angiogenesis only at the ischaemic myocardium but not at the normal myocardium in mice.[11] These results may represent the unique property of the LIPUS therapy that enhances an endogenous self-healing ability only in diseased tissues but not in normal tissues. Indeed, we have repeatedly noted this unique property of the LIPUS therapy, where increased susceptibility of diseased tissue to the cell surface molecules (e.g. caveolin-1) may be involved.[11–13]

In the present study, coronary microvascular endothelial function tended to be decreased in db/db mice and the LIPUS therapy improved it. It has been recently proposed that coronary microvascular dysfunction is closely related to cardiac diastolic dysfunction in HFpEF.[7] Since endothelial eNOS system plays an important role in regulating coronary microcirculation, up-regulated eNOS and its downstream pathway in response to LIPUS could improve microvascular function and ameliorate cardiac diastolic dysfunction. Indeed, in the present study, we demonstrated that LIPUS up-regulates eNOS and downstream molecules, such as sGC and PKG, but we were unable to detect significant increase in NO production in the myocardium (Supplementary material online, *Figure S9*). This suggests that other mechanisms could also contribute to the LIPUS-induced improvement of coronary microcirculation. We previously demonstrated that the eNOS system serves as the NO generating system in relatively large arteries, while it serves as the generating system of endothelium-dependent hyperpolarization (EDH) in microcirculation[43] and that EDH plays a crucial role in coronary microcirculation *in vivo*.[44] Recently, we also have demonstrated that EDH plays important roles in maintaining cardiac diastolic function *in vivo*.[23] Taken together, it is conceivable that the beneficial effect of LIPUS on cardiac diastolic dysfunction may be mediated, at least in part, through EDH up-regulation in coronary microcirculation.

4.5 Clinical implications

HFpEF is the most common type of HF and has been emerging as one of the most serious health problems worldwide.[3] Many clinical trials for HFpEF have failed to establish the effective therapy to improve the prognosis of HFpEF patients.[1,3] In the present study, based on our previous experiences with the LIPUS therapy,[10–12] we were able to demonstrate that our LIPUS therapy improves cardiac diastolic dysfunction and exercise tolerance in a mouse model of HFpEF. The power of LIPUS is controlled to keep the level lower below the upper limit of acoustic output standards (<720 mW/cm^2) for diagnostic ultrasound devices (US Food and Drug Administration's Track 3 Limits). In addition, since LIPUS directly emits low-intensity ultrasound to the heart from outside of the body, potential focal or systemic adverse effects should be minimal. Indeed, in the present study, no adverse effects were noted. In addition, we have previously demonstrated the efficacy and safety of our LIPUS

therapy with similar irradiation setting in a large animal (pig) model of chronic myocardial ischaemia.[10] Since HFpEF patients are often have various comorbidities, this minimally invasive feature of the LIPUS therapy appears to be important, suggesting that the LIPUS therapy could be a novel promising treatment for HFpEF patients.

4.6 Study limitations

Several limitations should be mentioned for the present study. First, in the present study, we showed the beneficial effect of the LIPUS therapy only in db/db mice, a mouse model of HFpEF associated with Type 2 DM.[32] Although DM is one of the most frequent comorbidities of HFpEF patients, there are a number of other background comorbidities that may contribute to the pathogenesis of HFpEF (e.g. hypertension, CKD, and chronic obstructive pulmonary disease). Thus, it remains to be examined whether our LIPUS therapy is also beneficial for other types of HFpEF. Second, in the present study, we showed the effectiveness of the LIPUS therapy in a 4-week treatment protocol. It is possible that the longer therapeutic period with the LIPUS therapy would achieve greater efficacy. This issue also remains to be examined in future studies. Third, in the present study, although we focused on the eNOS-NO-cGMP-PKG pathway as a main mechanism of the LIPUS-induced beneficial effects, other mechanisms may also be involved. Especially, regarding the antihypertrophic and antifibrotic effect of the LIPUS, its effects on neurohormonal factors, such as the renin–angiotensin–aldosterone system (RAAS), may possible.[45] Suppression of the RAAS may have attenuated LV remodelling (hypertrophy and fibrosis) and contributed to the reduction in LVEDP as confirmed by hemodynamic analysis, resulting in a reduction in serum BNP levels. This point remains be examined in future studies. Fourth, in the present study, although we demonstrated that the LIPUS therapy improved myocardial stiffness associated with suppression of myocardial hypertrophy and interstitial fibrosis, other factors, such as titin, may also be involved. Titin is a protein anchored to the sarcomere Z-line that serves as a major determinant of myocardial passive tension and stiffness.[46] The spring property is defined by the expression ratio of the cardiac isoforms N2B and N2BA and is modulated by its phosphorylation. It is known that PKG phosphorylates a target site of the N2B element, resulting in reduced passive tension.[47] Thus, in this viewpoint, it is possible that the LIPUS therapy would modulate the titin property by enhancing the eNOS-NO-cGMP-PKG pathway. This point remains be examined in future studies. Fifth, although LIPUS-treated db/db mice showed some evidence of reduced cardiac load (e.g. decreased LVEDP and lower levels of serum BNP), unexpectedly, it did not affect left arterial dimension evaluated by echocardiography (Supplementary material online, *Figure S2D*). This is possibly because the measurement was done only from parasternal long axis view, which is not necessarily appropriate method for evaluation of left atrial volume.[48] Other measurement modalities such as magnetic resonance imaging could provide more accurate measurement on left atrial dimension. Sixth, in invasive haemodynamic analysis, an open thorax preparation was used without fluid replacement. This might have led to lower performances and lower end-diastolic pressures in mice, although a series of measurements were performed under the same conditions in all animals. Seventh, in the present study, we demonstrated that LIPUS improves relaxation property at tissue level in the experiments using mouse trabeculae from the right ventricle. Although this technique with the right ventricular trabeculae has been widely used as an established experimental method to evaluate the electrophysiological properties of myocardial tissue,[17–19,49] caution should be paid when extrapolating the present finding to the left ventricle physiology. Eighth, in the present study, we evaluated exercise tolerance (capacity) using a work load calculated from treadmill running distance and body weight. However, for more appropriate evaluation of exercise capacity, it would be desirable to measure other parameters such as maximal oxygen uptake (VO_2 max) and anaerobic threshold (AT) by cardiopulmonary exercise testing (CPX) using an expired gas analyser. Ninth, since db/db mice had severe obesity with body weight about twice as much as control mice, this must be taken into account in the evaluation of some parameters. For example, in echocardiographic and haemodynamic analysis, correction by body surface area or body weight may be desirable. In addition, regarding serum BNP levels, the comparison between db/db mice and db/+ mice may not be simple because serum BNP levels are known to be lower in obese mice (e.g. db/db mice), just like in humans, in general.[50] Thus, in the present study, db/db mice may have lower BNP levels in comparison to the degree of cardiac dysfunction. Tenth, in the mouse trabeculae experiment, we used 4.0 mM of extracellular [Ca^{2+}], which was relatively higher than that of actual condition. Although we adopted this preparation in order to make it easier to evaluate the property of contraction and relaxation of the myocardium, physiological conditions have not been completely replicated.

5. Conclusions

In the present study, we were able to demonstrate that the LIPUS therapy ameliorates cardiac diastolic dysfunction in db/db mice through improvement of the eNOS-NO-cGMP-PKG pathway and cardiomyocyte Ca^{2+}-handling system without any side effects. Our results suggested that LIPUS may be a promising, new, non-invasive strategy for the treatment of HFpEF, for which there is no established therapy available. However, this concept has to be confirmed in humans.

Data availability

The data underlying this article will be shared on reasonable request to the corresponding author.

Supplementary material

Supplementary material is available at *Cardiovascular Research* online.

Authors' contributions

Y.M. performed most experiments and wrote the manuscript. T.S. and H.S. supervised the project and edited the manuscript. K.E., R.K., Y.K., Y.I., S.I., T.N., A.M., H.S., M.M., and H.K. designed or conducted experiments. S.M. performed analysing data.

Acknowledgements

We appreciate Y. Watanabe, H. Yamashita, and A. Nishihara for excellent technical supports.

Conflict of interest: none declared.

Funding

This research was supported by the Japan Society for the Promotion of Science (JSPS) (Grant No. 18K15877).

References

1. Shimokawa H, Miura M, Nochioka K, Sakata Y. Heart failure as a general pandemic in Asia. *Eur J Heart Fail* 2015;**17**:884–892.
2. Owan TE, Hodge DO, Herges RM, Jacobsen SJ, Roger VL, Redfield MM. Trends in prevalence and outcome of heart failure with preserved ejection fraction. *N Engl J Med* 2006;**355**:251–259.
3. Lourenço AP, Leite-Moreira AF, Balligand JL, Bauersachs J, Dawson D, de Boer RA, de Windt LJ, Falcão-Pires I, Fontes-Carvalho R, Franz S, Giacca M, Hilfiker-Kleiner D, Hirsch E, Maack C, Mayr M, Pieske B, Thum T, Tocchetti CG, Brutsaert DL, Heymans S. An integrative translational approach to study heart failure with preserved ejection fraction: a position paper from the Working Group on Myocardial Function of the European Society of Cardiology. *Eur J Heart Fail* 2018;**20**:216–227.
4. Margaret R, Steven J, John B, Douglas M, Kent B, Richard R. Burden of systolic and diastolic ventricular dysfunction in the community: appreciating the scope of the heart failure epidemic. *JAMA* 2013;**289**:194–202.
5. Paulus WJ, Tschope C. A novel paradigm for heart failure with preserved ejection fraction: comorbidities drive myocardial dysfunction and remodeling through coronary microvascular endothelial inflammation. *J Am Coll Cardiol* 2013;**62**:263–271.
6. Schiattarella GG, Altamirano F, Tong D, French KM, Villalobos E, Kim SY, Luo X, Jiang N, May HI, Wang ZV, Hill TM, Mammen PPA, Huang J, Lee DI, Hahn VS, Sharma K, Kass DA, Lavandero S, Gillette TG, Hill JA. Nitrosative stress drives heart failure with preserved ejection fraction. *Nature* 2019;**568**:351–356.
7. Crea F, Merz CNB, Beltrame JF, Kaski JC, Ogawa H, Ong P, Sechtem U, Shimokawa H, Camici P; COVADIS Group. The parallel tales of microvascular angina and heart failure with preserved ejection fraction: a paradigm shift. *Eur Heart J* 2017;**38**:473–477.
8. Triposkiadis F, Butler J, Abboud FM, Armstrong PW, Adamopoulos S, Atherton JJ, Backs J, Bauersachs J, Burkhoff D, Bonow RO, Chopra VK, de Boer RA, de Windt L, Hamdani N, Hasenfuss G, Heymans S, Hulot JS, Konstam M, Lee RT, Linke WA, Lunde IG, Lyon AR, Maack C, Mann DL, Mebazaa A, Mentz RJ, Nihoyannopoulos P, Papp Z, Parissis J, Pedrazzini T, Rosano G, Rouleau J, Seferovic PM, Shah AM, Starling RC, Tocchetti CG, Trochu JN, Thum T, Zannad F, Brutsaert DL, Segers VF, De Keulenaer GW. The continuous heart failure spectrum: moving beyond an ejection fraction classification. *Eur Heart* 2019;**40**:2155–2163.
9. Xin Z, Lin G, Lei H, Lue TF, Guo Y. Clinical applications of low-intensity pulsed ultrasound and its potential role in urology. *Transl Androl Urol* 2016;**5**:255–266.
10. Hanawa K, Ito K, Aizawa K, Shindo T, Nishimiya K, Hasebe Y, Tuburaya R, Hasegawa H, Yasuda S, Kanai H, Shimokawa H. Low-intensity pulsed ultrasound induces angiogenesis and ameliorates left ventricular dysfunction in a porcine model of chronic myocardial ischemia. *PLoS One* 2014;**9**:e104863.
11. Shindo T, Ito K, Ogata T, Hatanaka K, Kurosawa R, Eguchi K, Kagaya Y, Hanawa K, Aizawa K, Shiroto T, Kasukabe S, Miyata S, Taki H, Hasegawa H, Kanai H, Shimokawa H. Low-intensity pulsed ultrasound enhances angiogenesis and ameliorates left ventricular dysfunction in a mouse model of acute myocardial infarction. *Arterioscler Thromb Vasc Biol* 2016;**36**:1220–1229.
12. Ogata T, Ito K, Shindo T, Hatanaka K, Eguchi K, Kurosawa R, Kagaya Y, Monma Y, Ichijo S, Taki H, Kanai H, Shimokawa H. Low-intensity pulsed ultrasound enhances angiogenesis and ameliorates contractile dysfunction of pressure-overloaded heart in mice. *PLoS One* 2017;**12**:e0185555.
13. Eguchi K, Shindo T, Ito K, Ogata T, Kurosawa R, Kagaya Y, Monma Y, Ichijo S, Kasukabe S, Miyata S, Yoshikawa T, Yanai K, Taki H, Kanai H, Osumi N, Shimokawa H. Whole-brain low-intensity pulsed ultrasound therapy markedly improves cognitive dysfunctions in mouse models of dementia—crucial roles of endothelial nitric oxide synthase. *Brain Stim* 2018;**11**:959–973.
14. Hamdani N, Hervent AS, Vandekerckhove L, Matheeussen V, Demolder M, Baerts L, De Meester I, Linke WA, Paulus WJ, De Keulenaer GW. Left ventricular diastolic dysfunction and myocardial stiffness in diabetic mice is attenuated by inhibition of dipeptidyl peptidase 4. *Cardiovasc Res* 2014;**104**:423–431.
15. Methawasin M, Strom JG, Slater RE, Fernandez V, Saripalli C, Granzier H. Experimentally increasing the compliance of titin through RNA binding motif-20 (RBM20) inhibition improves diastolic function in a mouse model of heart failure with preserved ejection fraction. *Circulation* 2016;**134**:1085–1099.
16. Flecknell PA. *Laboratory Animal Anesthesia*. 3rd ed. Burlington, MA: Academic Press; 2008.
17. Miura M, Wakayama Y, Endoh H, Nakano M, Sugai Y, Hirose M, Ter Keurs HE, Shimokawa H. Spatial non-uniformity of excitation-contraction coupling can enhance arrhythmogenic-delayed afterdepolarizations in rat cardiac muscle. *Cardiovasc Res* 2008;**80**:55–61.
18. Miura M, Nishio T, Hattori T, Murai N, Stuyvers BD, Shindoh C, Boyden PA. Effect of nonuniform muscle contraction on sustainability and frequency of triggered arrhythmias in rat cardiac muscle. *Circulation* 2010;**121**:2711–2717.
19. Sunamura S, Satoh K, Kurosawa R, Ohtsuki T, Kikuchi N, Elias-Al-Mamun M, Shimizu T, Ikeda S, Suzuki K, Satoh T, Omura J, Nogi M, Numano K, Siddique MAH, Miyata S, Miura M, Shimokawa H. Different roles of myocardial ROCK1 and ROCK2 in cardiac dysfunction and postcapillary pulmonary hypertension in mice. *Proc Natl Acad Sci USA* 2018;**115**:E7129–E7138.
20. Godo S, Sawada A, Saito H, Ikeda S, Enkhjargal B, Suzuki K, Tanaka S, Shimokawa H. Disruption of physiological balance between nitric oxide and endothelium-dependent hyperpolarization impairs cardiovascular homeostasis in mice. *Arterioscler Thromb Vasc Biol* 2016;**36**:97–107.
21. Saito H, Godo S, Sato S, Ito A, Ikumi Y, Tanaka S, Ida T, Fujii S, Akaike T, Shimokawa H. Important role of endothelial caveolin-1 in the protective role of endothelium-dependent hyperpolarization against nitric oxide-ediated nitrative stress in microcirculation in mice. *J Cardiovasc Pharmacol* 2018;**71**:113–126.
22. Ikumi Y, Shiroto T, Godo S, Saito H, Tanaka S, Ito A, Kajitani S, Monma Y, Miyata S, Tsutsui M, Shimokawa H. Important roles of endothelium-dependent hyperpolarization in coronary microcirculation and cardiac diastolic function in mice. *J Cardiovasc Pharmacol* 2020;**75**:31–40.
23. Konietschke F, Placzek M, Schaarschmidt F, Hothorn LA. Nparcomp: an R software package for nonparametric multiple comparisons and simultaneous confidence intervals. *J Stat Software* 2015;**61**:1–17.
24. Mohammed SF, Hussain S, Mirzoyev SA, Edwards WD, Maleszewski JJ, Redfield MM. Coronary microvascular rarefaction and myocardial fibrosis in heart failure with preserved ejection fraction. *Circulation* 2015;**131**:550–559.
25. Butler J, Fonarow GC, Zile MR, Lam CS, Roessig L, Schelbert EB, Shah SJ, Ahmed A, Bonow RO, Cleland JG, Cody RJ, Chioncel O, Collins SP, Dunnmon P, Filippatos G, Lefkowitz MP, Marti CN, McMurray JJ, Misselwitz F, Nodari S, O'Connor C, Pfeffer MA, Pieske B, Pitt B, Rosano G, Sabbah HN, Senni M, Solomon SD, Stockbridge N, Teerlink JR, Georgiopoulou VV, Gheorghiade M. Developing therapies for heart failure with preserved ejection fraction: current state and future directions. *JACC Heart Fail* 2014;**2**:97–112.
26. Pereira L, Ruiz-Hurtado G, Rueda A, Mercadier J-J, Benitah J-P, Gómez AM. Calcium signaling in diabetic cardiomyocytes. *Cell Calcium* 2014;**56**:372–380.
27. van der Velden J, Stienen G. Cardiac disorders and pathophysiology of sarcomeric proteins. *Physiol Rev* 2019;**99**:381–426.
28. McHugh K, DeVore AD, Wu J, Matsouaka RA, Fonarow GC, Heidenreich PA, Yancy CW, Green JB, Altman N, Hernandez AF. Heart failure with preserved ejection fraction and diabetes: JACC State-of-the-Art Review. *J Am Coll Cardiol* 2019;**73**:602–611.
29. Echouffo-Tcheugui JB, Xu H, DeVore AD, Schulte PJ, Butler J, Yancy CW, Bhatt DL, Hernandez AF, Heidenreich PA, Fonarow GC. Temporal trends and factors associated with diabetes mellitus among patients hospitalized with heart failure: findings from Get With The Guidelines-Heart Failure registry. *Am Heart J* 2016;**182**:9–20.
30. Takeda Y, Sakata Y, Mano T, Ohtani T, Kamimura D, Tamaki S, Omori Y, Tsukamoto Y, Aizawa Y, Komuro I, Yamamoto K. Competing risks of heart failure with preserved ejection fraction in diabetic patients. *Eur J Heart Fail* 2011;**13**:664–669.
31. Sandesara PB, O'Neal WT, Kelli HM, Samman-Tahhan A, Hammadah M, Quyyumi AA, Sperling LS. The prognostic significance of diabetes and microvascular complications in patients with heart failure with preserved ejection fraction. *Diabetes Care* 2018;**41**:150–155.
32. Conceicao G, Heinonen I, Lourenco AP, Duncker DJ, Falcao-Pires I. Animal models of heart failure with preserved ejection fraction. *Neth Heart J* 2016;**24**:275–286.
33. Reil JC, Hohl M, Reil GH, Granzier HL, Kratz MT, Kazakov A, Fries P, Muller A, Lenski M, Custodis F, Graber S, Frohlig G, Steendijk P, Neuberger HR, Bohm M. Heart rate reduction by If-inhibition improves vascular stiffness and left ventricular systolic and diastolic function in a mouse model of heart failure with preserved ejection fraction. *Eur Heart J* 2013;**34**:2839–2849.
34. Roh J, Houstis N, Rosenzweig A. Why don't we have proven treatments for HFpEF? *Circ Res* 2017;**120**:1243–1245.
35. Parton RG. Life without caveolae. *Science* 2001;**293**:2404–2405.
36. Ingber DE, Tensegrity II. How structural networks influence cellular information processing networks. *J Cell Sci* 2003;**116**:1397–1408.
37. Takimoto E, Champion HC, Li M, Belardi D, Ren S, Rodriguez ER, Bedja D, Gabrielson KL, Wang Y, Kass D. Chronic inhibition of cyclic GMP phosphodiesterase 5A prevents and reverses cardiac hypertrophy. *Nat Med* 2005;**11**:214–222.
38. Xue M, Li T, Wang Y, Chang Y, Cheng Y, Lu Y, Liu X, Xu L, Li X, Yu X, Sun B, Chen L. Empagliflozin prevents cardiomyopathy via sGC-cGMP-PKG pathway in type 2 diabetes mice. *Clin Sci (Lond)* 2019;**133**:1705–1720.
39. Matyas C, Nemeth BT, Olah A, Torok M, Ruppert M, Kellermayer D, Barta BA, Szabo G, Kokeny G, Horvath EM, Bodi B, Papp Z, Merkely B, Radovits T. Prevention of the development of heart failure with preserved ejection fraction by the phosphodiesterase-5A inhibitor vardenafil in rats with type 2 diabetes. *Eur J Heart Fail* 2017;**19**:326–336.
40. Wang D, Shan Y, Huang Y, Tang Y, Chen Y, Li R, Yang J, Huang C. Vasostatin-1 stops structural remodeling and improves calcium handling via the eNOS-NO-PKG pathway in rat hearts subjected to chronic beta-adrenergic receptor activation. *Cardiovasc Drugs Ther* 2016;**30**:455–464.
41. Bers DM. Calcium cycling and signaling in cardiac myocytes. *Annu Rev Physiol* 2008;**70**:23–49.
42. Frantz S, Klaiber M, Baba HA, Oberwinkler H, Völker K, Gaßner B, Bayer B, Abeßer M, Schuh K, Feil R, Hofmann F, Kuhn M. Stress-dependent dilated cardiomyopathy in mice with cardiomyocyte-restricted inactivation of cyclic GMP-dependent protein kinase I. *Eur Heart J* 2013;**34**:1233–1244.

43. Shimokawa H. 2014 Williams Harvey Lecture: importance of coronary vasomotion abnormalities-from bench to bedside. *Eur Heart J* 2014 ;**35**:3180–3193.
44. Yada T, Shimokawa H, Hiramatsu O, Shinozaki Y, Mori H, Goto M, Ogasawara Y, Kajiya F. Important role of endogenous hydrogen peroxide in pacing-induced metabolic coronary vasodilation in dogs *in vivo*. *J Am Coll Cardiol* 2007;**50**:1272–1278.
45. Weber KT, Brilla CG. Pathological hypertrophy and cardiac interstitium. Fibrosis and renin-angiotensin-aldosterone system. *Circulation* 1991;**83**:1849–1865.
46. Zile MR, Baicu CF, S. Ikonomidis J, Stroud RE, Nietert PJ, Bradshaw AD, Slater R, Palmer BM, Van Buren P, Meyer M, M. Redfield M, A. Bull D, L. Granzier H, LeWinter MM. Myocardial stiffness in patients with heart failure and a preserved ejection fraction: contributions of collagen and titin. *Circulation* 2015;**131**:1247–1259.
47. Kötter S, Gout L, Von Frieling-Salewsky M, Müller AE, Helling S, Marcus K, Dos Remedios C, Linke WA, Krüger M. Differential changes in titin domain phosphorylation increase myofilament stiffness in failing human hearts. *Cardiovasc Res* 2013;**99**:648–656.
48. Lester SJ, Ryan EW, Schiller NB, Foster E. Best method in clinical practice and in research studies to determine left atrial size. *Am J Cardiol* 1999;**84**:829–832.
49. Schillinger W, Teucher N, Sossalla S, Kettlewell S, Werner C, Raddatz D, Elgner A, Tenderich G, Pieske B, Ramadori G, SchöNdube FA, KöGler H, KockskäMper J, Maier LS, SchwöRer H, Smith GL, Hasenfuss G. Negative inotropy of the gastric proton pump inhibitor pantoprazole in myocardium from humans and rabbits: evaluation of mechanisms. *Circulation* 2007;**116**:57–66.
50. Bartels ED, Nielsen JM, Bisgaard LS, Goetze JP, Nielsen LB. Decreased expression of natriuretic peptides associated with lipid accumulation in cardiac ventricle of obese mice. *Endocrinology* 2010;**151**:5218–5225.

Translational perspective

Although heart failure with preserved left ventricular ejection fraction (HFpEF) is a serious health problem worldwide, no effective treatment is yet available. We have previously demonstrated that our low-intensity pulsed ultrasound (LIPUS) therapy is effective and safe in animal models of angina and dementia. In this study, we examined whether our LIPUS therapy is also effective to improve cardiac diastolic dysfunction in mice. We found that the LIPUS therapy ameliorated myocardial structures and Ca^{2+}-handling proteins, resulting in the improvement of cardiac diastolic functions and exercise tolerance in a mouse model of HFpEF. These results suggest that the LIPUS therapy is useful for the treatment of HFpEF in humans.